15th International Particle Accelerator Conference,Nashville, TN JACoW Publishing
ISBN: 978-3-95450-247-9 ISSN: 2673-5490 doi: 10.18429/JACoW-IPAC2024-TUPS17

LONGITUDINAL PHASE SPACE MEASUREMENTS AT MedAustron

K. Holzfeind*, F. Kühteubl, E. Renner, TU Wien, Vienna, Austria
L. Fischl, G. Guidoboni, C. Kurfürst, C. Maderböck, F. Plassard, D. Prokopovich, C. Schmitzer,
A. Wastl, M. Wolf, EBG MedAustron GmbH, Wr. Neustadt, Austria

Abstract

MedAustron is an ion therapy facility located in Wiener Neustadt, Austria, which uses third order resonant slow extraction to deliver protons and carbon ions for clinical irradiation. The foreseen upgrade of the new low level RF (LLRF) system facilitates advanced longitudinal beam manipulation schemes involving multiple RF harmonics, which will be exploited to improve the slow extraction process and the consequent spill characteristics. To support these studies and provide a new diagnostic tool longitudinal tomography is being implemented. This proceeding presents the employed measurement set-ups and compares the first obtained tomographic reconstructions with BLonD simulations.

INTRODUCTION

The synchrotron-based centre for ion beam therapy and research MedAustron (Wiener Neustadt, Austria) performs cancer treatments using proton and carbon ion beams with energies between 62-252 MeV and 120-402 MeV/u, respectively. The beam can be delivered to four irradiation rooms, three for clinical treatment and one room for non-clinical research (NCR) studies of academic users. In addition to the clinical beams, special beam types, including proton beams up to 800 MeV, low-flux [1] and helium ion beams [2], are delivered to this dedicated NCR room.

Foreseen upgrades of the synchrotron's low-level radio frequency (LLRF) system motivate the expansion of diagnostics tools for the longitudinal phase space. So far, longitudinal bunch diagnostics had been available through momentum distribution measurements using the Schottky monitor and empty bucket-measuremetns [3]. To broaden these possibilities, efforts to profit of turn-by-turn measurements of longitudinal bunch profiles as well as longitudinal tomography are in progress. In addition to its potential in aiding the multi-harmonic operation offered by the new LLRF system, longitudinal tomography will also be beneficial for the ongoing investigations of alternative extraction mechanisms at MedAustron [4], particularly when exploring the slow extraction of bunched beams and multi-energy extraction.

The first part of the paper provides a brief overview of the RF program applied at MedAustron, the available longitudinal bunch diagnostics and the foreseen LLRF system upgrade. The second part presents simulation and measurement results of the first longitudinal phase space reconstructions using the newly developed set-up.

* katrin.holzfeind@chello.at

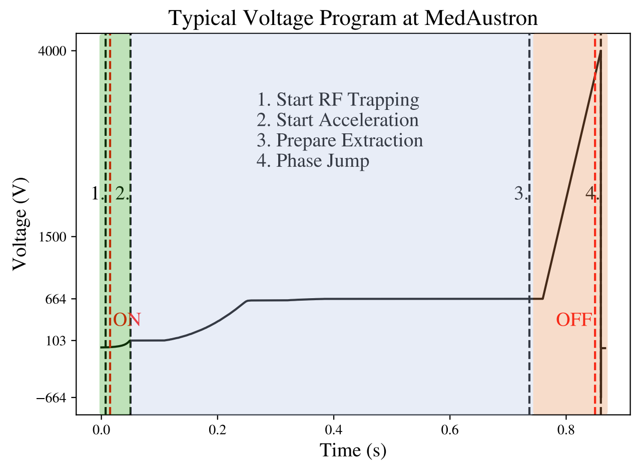

Figure 1: RF voltage program of a typical 252 MeV proton cycle. The red lines show the activation and deactivation of radial and phase loop. The loops are turned off before the phase jump. Green region: injection and capture; blue: acceleration, red: flat top and extraction preparation.

SYSTEM LAYOUT

Synchrotron RF Program at MedAustron

The RF voltage program of a 252 MeV proton cycle is illustrated in Fig. 1. The beam is injected into the synchrotron at ≈7 Mev/u via multi-turn injection. The momentum spread $\delta=\Delta p/p$ of the injected beam can be regulated using a debuncher cavity located in the beam transfer line between the LINAC and the injection system. The coasting beam is captured using a fixed synchrotron RF-frequency, while maintaining a constant magnetic field. After a delay of some milliseconds, radial and phase loop are turned on to regulate the RF frequency.

At the beginning of the acceleration the bucket voltage is chosen to compromise longitudinal and transverse losses. In order to minimise longitudinal losses the bucket area should remain constant, to counteract the separatrix closing. At the same time transverse losses due to the increasing momentum spread and related dispersive beam size have to be considered.

For clinical application, the slow extraction is driven by a betatron core, which requires a large quasi-uniform momentum spread. This is achieved by performing an 180° phase jump (marker 4. in Fig. 1). After the phase jump, the beam expands from the unstable fixed point along the separatrix, which increases the rms momentum spread from $\delta_{\mathrm{rms}}\approx 0.035$ up to ≈0.15%. To attain this specified momentum spread, an initial increase of the momentum spread is already introduced prior to the phase jump by linearly increasing the

ISBN: 978-3-95450-247-9 ISSN: 2673-5490 doi: 10.18429/JACoW-IPAC2024-TUPS17

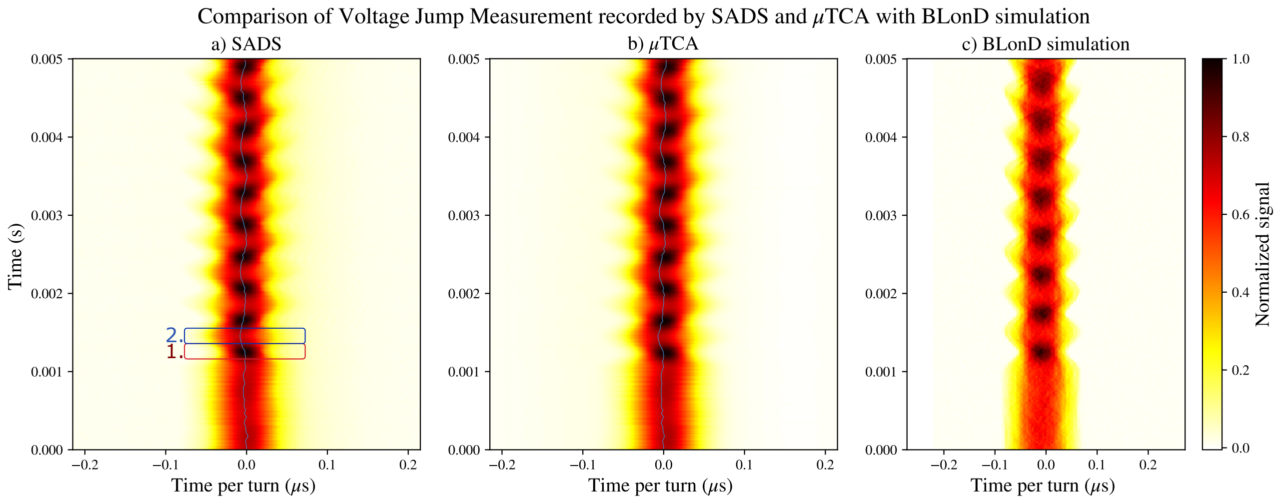

Figure 2: Waterfall diagrams, when instantaneously increasing the bucket voltage from the nominal 663 V to 1500 V. The profiles are acquired with the a) SADS, the b) μTCA-crate and c) BLonD simulations. The symmetry point of each turn is visualized in blue. The red box indicates a time interval, during which the beam has a small bunch length and large momentum spread δ . The beam subsequently rotates in phase space, increasing the length and decreasing δ (blue box).

bucket voltage, i.e. from below 700 to approx. 4000 V for 252 MeV protons (between markers 3 and 4 in Fig. 1). For the lowest proton extraction energy (62 MeV) and carbon beams this voltage ramp is not required and thus not applied. Subsequently, the RF is turned off to unbunch the beam. During the extraction process, empty bucket channelling is used to reduce spill ripples [5].

Hardware and Foreseen Upgrades

The existing LLRF system utilizes standard orbit pick-ups to verify the single harmonic operation of the synchrotron. The turn-by-turn longitudinal profiles, necessary for the tomographic reconstruction, are measured with the same orbit pick-ups as are used for the LLRF control. The induced voltage can be recorded using two acquisition systems, the so-called *Signal Acquisition and Distribution System* (SADS) or a new Micro Telecommunications Computing Architecture (μTCA)-based measurement crate. The SADS is designed for acquiring, processing, and observing analogue signals efficiently. It comprises three oscilloscopes linked to the Main Timing System and signal routing control. This configuration enables users to choose from a pool of 144 analogue signals with a frequency range of 50 MHz, along with 8 analogue signals with a frequency range of 500 MHz. However, as the components of the LLRF approach the end of their operational lifespan and the need for higher harmonic operation arises, a new LLRF system will be introduced. The μTCA-based system, described in reference [6], will be used for beam measurements required for the new LLRF system in the injector and the synchrotron at MedAustron. It is capable of sampling orbit pick-ups (or other) data at rates up to 1 GSps and a frequency range of 400 kHz to 500 MHz. It can be used as a digitizer storing up to ~ 60 ms of raw ADC data at the highest sampling rate, or it can preprocess and demodulate signals for easy beam phase and position measurements. The direct sampling mode will be used to acquire data for offline tomography calculations.

LONGITUDINAL TOMOGRAPHY

The possibility to reconstruct the longitudinal phase space offers a new diagnostic tool, which is beneficial for the ongoing extraction studies and will be essential for exploiting the multi-harmonic capabilities provided by the new LLRF system. A well-established code for tomographic reconstruction of the longitudinal phase space is provided by CERN [7, 8]. The iterative algorithm requires the acquired turn-by-turn longitudinal profiles and information on the machine state during the measurements as input.

Methods

To assess the long-term suitability of the two described acquisition systems for providing data in a longitudinal tomography setup, systematic measurements are being performed for various energies, particle types and intensities and compared to BLonD [9] simulations. These tests are being performed for nominal cycles as well as under specifically introduced RF manipulations, e. g. frequency or voltage jumps. As a raw signal we use the sum signal of a horizontal orbit pick-up, recorded simultaneously with both acquisition systems. The SADS can record the RF voltage in parallel, a functionality which has yet to be implemented for the μTCA-crate.

As an illustrative example, this section presents measurements and simulations of the longitudinal phase space evolution when introducing a non-nominal voltage increase from the nominal bucket voltage of 663.52 to 1500 V, which increases the bucket height by 50%. The measurements are taken for a stationary 252 MeV proton beam at flat top (FT).

ISBN: 978-3-95450-247-9 ISSN: 2673-5490 doi: 10.18429/JACoW-IPAC2024-TUPS17

Results and Discussion

Figure 2 shows the waterfall diagrams obtained from the measurements and simulations. Both acquisition systems clearly display the expected quadrupolar-mode oscillation, which is initiated by the applied voltage jump as the longitudinal distribution no longer matches the bucket shape. The time intervals corresponding to both long and short bunch lengths or small and large momentum spread, respectively, are indicated in Fig. 2 with a blue and red box. The individual turns are isolated from the acquired raw signal by using the RF voltage from the SADS as a reference, i. e. considering phases between $\Phi \in [-\pi, \pi)$ from the zero crossing of the RF voltage. To enhance the illustration, the blue line indicates the symmetry point, which is calculated for each turn by finding the phase Φ_1, which minimizes

$$\Delta = \left| \sum_{\Phi_1-\pi}^{\Phi_1} f(\Phi) - \sum_{\Phi_1}^{\Phi_1+\pi} f(\Phi) \right|, \quad (1)$$

with $f(\Phi)$ being the pick-up signal at phase Φ [10].

Qualitatively, both acquisition systems offer comparable performance, yielding similar results for the tomography as well. As example, the reconstructed phase space based on the µTCA-crate measurements is illustrated in Fig. 3 for a time instance with large momententum spread and small bunch length (red box in Fig. 2).

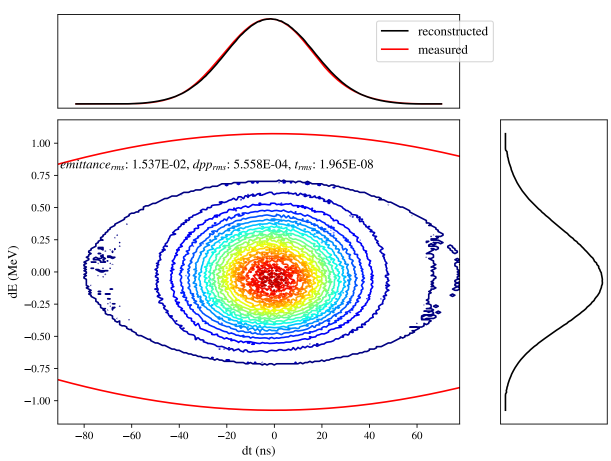

Figure 3: Reconstructed phase space based on the profiles acquired with the µTCA-crate, featuring a time instance with large momentum spread and small bunch length.

Table 1: Reconstructed Beam Parameters in Region 1

	ϵ_L [10^{-2} eVs]	δ_{rms} [10^{-4}]	Bunch length [ns]
µTCA	1.54	5.56	79
SADS	1.83	5.81	90
r.BLonD	1.66	5.48	87
BLonD	1.69	5.57	86

Table 2: Reconstructed Beam Parameters in Region 2

	ϵ_L [10^{-2} eVs]	δ_{rms} [10^{-4}]	Bunch length [ns]
µTCA	1.54	4.05	108
SADS	1.81	4.54	114
r.BLonD	1.65	3.70	126
BLonD	1.69	3.72	129

For a more in-depth comparison, the longitudinal emittance ϵ_L, δ_{rms} and the bunch length l are computed from the tomographic reconstruction for both systems. Tables 1 and 2 list the results for the oscillation phases featuring large and small momentum spread, respectively (red and blue box in Fig. 2). The computed beam parameters are compared to BLonD simulations. To enhance the comparison, tomography is performed using the simulated turn-by-turn profiles, labelled by 'r.BLonD' in Tables 2 and 1. There are still quantitative differences between the two measurement setups and the simulations, which will be investigated in follow-up studies. However, there is a consistent overall trend across all cases portraying the quadrupolare-mode oscillations, which is evident when computing for each case the relative variation of the beam parameters between region 1 and 2 (Table 3). It is noteworthy that the impact of the introduced voltage jump is more pronounced in both the simulation and its reconstruction (momentum spread variation of ≈50 %) than in the measurements (≈28-37 %) as seen in Table 3. This difference is currently under investigation. As the beam has not started filamenting yet, no significant difference in emittance is obtained in either case.

Table 3: Relative Difference Between Region 1 and 2

	$\frac{\Delta\epsilon}{\epsilon}$	$\frac{\Delta\delta_{rms}}{\delta_{rms}}$	$\frac{\Delta l}{l}$
µTCA	-0.07 %	-37 %	27 %
SADS	-0.7 %	-28 %	21 %
r.BLonD	-0.6 %	-47 %	32 %
BLonD	-0.01 %	-50 %	33 %

CONCLUSION

Longitudinal tomography, as provided by the CERN code, has been adapted to MedAustron's specifications and offers a reliable reconstruction of the longitudinal phase space. Further studies of beam dynamics, including bunched beam and multi-energy extraction, at MedAustron will now be assisted by tomography.

ACKNOWLEDGMENTS

The authors want to thank the non-clinical research users and the MTA and OPS departments at EBG MedAustron Research and Treatment center for their support.

ISBN: 978-3-95450-247-9 ISSN: 2673-5490 doi: 10.18429/JACoW-IPAC2024-TUPS17

REFERENCES

[1] F. Ulrich-Pur *et al.*, “Commissioning of low particle flux for proton beams at MedAustron”, *Nucl. Instrum. Methods A*, vol. 1010, p. 165 570, Sep. 2021. doi:10.1016/j.nima.2021.165570

[2] M. Kausel *et al.*, “Injector and synchrotron commissioning of helium ion beams at the medaustron ion therapy center”, in *Proc. IPAC'23*, Venice, Italy, May 2023, pp. 1713–1716. doi:10.18429/JACoW-IPAC2023-TUPA175

[3] C. Schmitzer *et al.*, “MedAustron Synchrotron RF Commissioning for Medical Proton Beams”, in *Proc. IPAC'16*, Busan, Korea, Jun. 2016, pp. 844–846. doi:doi:10.18429/JACoW-IPAC2016-MOPOY001

[4] F. Kuehteubl *et al.*, “Investigating alternative extraction methods at medaustron”, in *Proc. IPAC'23*, Venice, Italy, May 2023, pp. 2419–2422. doi:10.18429/JACoW-IPAC2023-TUPM091

[5] A. De Franco *et al.*, “Slow extraction optimization at the MedAustron ion therapy center: Implementation of front end acceleration and rf knock out”, in *Proc. IPAC'18*, Vancouver, BC, Canada, Jun. 2018, pp. 453–456. doi:10.18429/JACoW-IPAC2018-MOPML025

[6] M. Wolf *et al.*, “Development and integration of a new low-level RF system for MedAustron”, in *Proc. LINAC'22*, Liverpool, UK, Sep. 2022, paper THPOPA12, pp. 764–766. doi:10.18429/JACoW-LINAC2022-THPOPA12

[7] S. Hancock, “A simple algorithm for longitudinal phase space tomography”, CERN, Geneva, Switzerland, Rep. CERN-PS-RF-NOTE-97-06, May 1997.

[8] C. H. Grindheim and S. Albright, “Longitudinal phase space tomography version 3”, CERN, Geneva, Switzerland, Rep. CERN-ACC-Note-2021-0004, Jan. 2021.

[9] H. Timko, J. Esteban Müller, A. Lasheen, and D. Quartullo, “Benchmarking the Beam Longitudinal Dynamics Code BLonD”, in *Proc. IPAC'16*, Busan, Korea, Jun. 2016, pp. 3094–3097. doi:10.18429/JACoW-IPAC2016-WEPOY045

[10] D. Kelliher *et al.*, “Longitudinal Tomography in a Scaling FFA”, in *Proc. IPAC'19*, Melbourne, Australia, Jun. 2019, pp. 719–722. doi:10.18429/JACoW-IPAC2019-MOPRB063